



OPEN

DATA DESCRIPTOR

Quantum chemical calculations for over 200,000 organic radical species and 40,000 associated closed-shell molecules

Peter C. St. John¹✉, Yanfei Guan², Yeonjoon Kim¹, Brian D. Etz¹, Seonah Kim¹✉ & Robert S. Paton³✉

The stabilities of radicals play a central role in determining the thermodynamics and kinetics of many reactions in organic chemistry. In this data descriptor, we provide consistent and validated quantum chemical calculations for over 200,000 organic radical species and 40,000 associated closed-shell molecules containing C, H, N and O atoms. These data consist of optimized 3D geometries, enthalpies, Gibbs free energy, vibrational frequencies, Mulliken charges and spin densities calculated at the M06-2X/def2-TZVP level of theory, which was previously found to have a favorable trade-off between experimental accuracy and computational efficiency. We expect this data to be useful in the further development of machine learning techniques to predict reaction pathways, bond strengths, and other phenomena closely related to organic radical chemistry.

Background & Summary

Accurate determination of reaction energies is a central step in exploring organic chemistry mechanisms. The majority of chemical reactions consist of multiple elementary steps involving reactive intermediates. Short-lived reactive intermediates are difficult to isolate and analyze experimentally, resulting in increased dependence on accurate mechanistic insight gained from computational techniques¹. Calculating reaction energies with quantum chemistry techniques, such as density functional theory (DFT), is therefore a central effort of computational organic chemistry. However, the combinatorial complexity of potential reaction pathways requires significant experience on the part of the computational chemist to determine which pathways are most likely to be feasible, and considerable computational resources to ensure enough pathways are explored that nonintuitive reactive intermediates and products are not missed. Enthalpies of radicals in particular, as important intermediates in combustion^{2,3}, atmospheric⁴, redox⁵, (bio)-polymer chemistry^{6,7}, and the functionalization of medicinally-relevant aromatic compounds⁸, are frequently calculated to determine the thermodynamics and kinetics of reaction pathways. Fast and accurate predictions for the enthalpy changes of radical reactions will substantially improve the throughput of computational chemistry research and allow detailed calculations to be targeted towards pathways that have the highest likelihood of being experimentally relevant.

The accuracy of Machine Learning (ML) models in predicting the results of quantum mechanical calculations has increased substantially in recent years as techniques for connecting molecular structures to deep neural networks have improved^{9–11}. These approaches, known as graph neural networks (GNNs)¹², replace the traditional featurization of molecules using fingerprints or descriptors with a framework in which molecular representations are learned from the underlying data¹³. These frameworks therefore continue to increase in accuracy as more data is collected far beyond traditional machine learning approaches. ML approaches to quickly and accurately predict enthalpy¹⁴, ground state energy¹⁵, bond dissociation energy¹⁶, and even transition-state activation energies¹⁷ have been developed by leveraging increasingly large databases of DFT calculations. The public distribution of large quantum chemistry databases, such as ioChem-BD¹⁸, is an important part of advancing the field of

¹Biosciences Center, National Renewable Energy Laboratory, 15103 Denver West Parkway, Golden, Colorado, 80401, United States. ²Department of Chemical Engineering, Massachusetts Institute of Technology, 77 Massachusetts Ave., Cambridge, MA, 02139, USA. ³Department of Chemistry, Colorado State University, Fort Collins, Colorado, 80523, USA. ✉e-mail: peter.stjohn@nrel.gov; seonah.kim@nrel.gov; robert.paton@colostate.edu

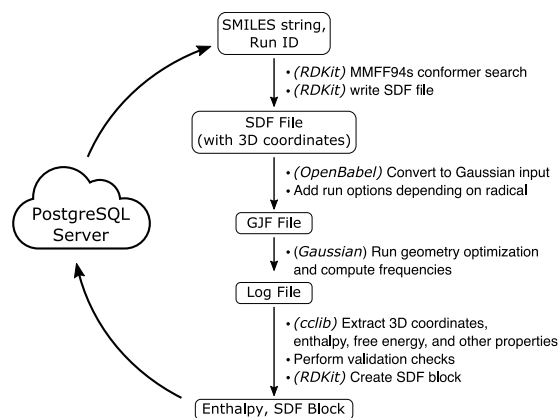


Fig. 1 Overview of the calculation pipeline and associated software. On each worker, closed-shell molecules and radicals (in SMILES format) are pulled from a central database. Optimized, validated 3D geometries are stored in the database after completed, and a new molecule is started.

machine learning research in computational chemistry, as prior publications of equilibrium¹⁹, off-equilibrium²⁰, and transition-state structures²¹ have found applicability beyond their original purpose. Datasets such as QM7²², QM9¹⁹, ANI-1x²³, and ANI-1ccx²⁴ consist of closed-shell organic molecules and so a dataset containing reactive intermediates, such as radical species, is required for the further development of machine learning models.

In this data descriptor, we report a quantum chemistry dataset focused on determining the enthalpies of radical reactions for small organic molecules. The database contains over 200,000 organic radical species and more than 40,000 associated closed-shell molecules, which were generated by breaking single, non-cyclic bonds in molecules taken from the PubChem Compound database²⁵. Carbon, nitrogen and oxygen centered radicals are represented. Geometry optimizations and enthalpy calculations were performed at the M06-2X/def2-TZVP level of theory²⁶, which was previously found to have a favorable trade-off between experimental accuracy and computational efficiency. For calculating the bond dissociation enthalpies specifically, results from this DFT methodology were benchmarked against experimental bond dissociation energies and calculations at higher levels of theory¹⁶. The calculation pipeline showed similar performance to CCSD(T), and is able to capture changes in enthalpy relative to experiment with an accuracy of approximately 2 kcal mol⁻¹.

The resulting database consists of optimized 3D geometries, vibrational frequencies, IR intensities, Mulliken atomic charges, spin densities, enthalpies and free energies for each molecule, calculated using Gaussian 16²⁷. While this data was developed primarily for calculating bond strengths of organic molecules²⁸, we expect this comprehensive database of radical and closed-shell calculations to be useful for a wide range of applications in chemistry.

Methods

Selection of closed-shell molecules and radicals. SMILES strings for closed-shell molecules were selected from the PubChem Compound database²⁵ where the entry had a valid CAS number, ten or fewer heavy atoms, consisted of only C, H, N, and O atoms, did not contain formal charges on any atoms, and for which all atoms were connected via covalent bonds (i.e., entries containing multiple molecules or ionic bonds were removed). From these parent molecules, SMILES strings for child radicals were generated by iteratively breaking all single, non-ring bonds in the parent molecule. The resulting list of SMILES strings was canonicalized and de-duplicated using RDKit²⁹.

Conformer optimization. An initial guess for the lowest-energy conformer was performed via a search using the MMFF94s force-field, as implemented in RDKit³⁰. The number of sampled conformers was determined by min (max (3^{*n*}, 100), 1000), where *n* is the number of rotatable bonds in the molecule. The lowest-energy conformer was then used as the initial geometry guess for subsequent DFT calculations. In order to obtain realistic geometry guesses for radical species (on which MMFF94s was not parameterized), H-atoms were added to radical centers prior to conformer generation. Basic knowledge of chemical structure, including ring conformations, was also incorporated into initial guesses for conformer structure³¹.

Density functional theory calculations. Gaussian input files were created from the lowest-energy conformer using OpenBabel³². DFT calculations were performed using Gaussian 16²⁷ with the M06-2X functional and def2-TZVP basis set with the default ultra-fine grid for all numerical integrations. For radical calculations, additional care was taken to ensure the correct electronic structure. Specifically, spatial and spin symmetry of orbitals were broken through an initial guess of mixed HOMO-LUMO and assuming no point-group symmetry. Stability of the DFT “wavefunction” was also tested, and the geometry was reoptimized if an instability was found. Results were parsed in Python using the cclib package³³.

Parallel QM calculations. Calculations were distributed across a high-performance computing (HPC) cluster (Fig. 1). A PostgreSQL database was used to coordinate calculations for a pool of worker nodes. Each worker,

Data Field	Description
SMILES	String representation of the 2D connectivity of the molecule. Radicals are denoted using the bracket notation.
Enthalpy	Molecular enthalpies, specified to six decimal places. In Hartree
FreeEnergy	Gibbs energy at standard temperature (298.15 K) and pressure (1 atm). In Hartree
SCFenergy	Total SCF energy (electronic + nuclear). In Hartree
AtomCharges	Mulliken atomic charges, one for each atom. The values are formatted as a python list, beginning and ending with brackets and separated with commas. Values correspond to the atom order as given in the 3D coordinates.
AtomSpins	Atomic spin densities (for radicals only). In the same format as AtomCharges.
VibFreqs	Vibrational frequencies in wavenumbers (cm^{-1}). Formatted as a python list of length 3N-6 (or 3N-5 for linear molecules)
RotConstants	Rotational constants (GHz). A formatted python list of length 3.
IRIntensity	Infrared intensities (km/mol). In the same format as VibFreqs.

Table 1. Description of the associated data fields, their formats, and units.

# Heavy Atoms	Molecules	Radicals
0	0	1
1	3	4
2	11	17
3	50	89
4	167	404
5	485	1867
6	1326	6570
7	3452	19931
8	7573	46163
9	13594	86499
10	16615	84818

Table 2. Number of optimized closed-shell molecules and radicals by number of heavy atoms.

Element	Primary	Secondary	Tertiary
C	56,067	121,369	28,135
N	11,349	14,048	
O	15,354		

Table 3. Distribution of the 246,363 radicals by location of the unpaired electron. Primary, secondary, and tertiary refers to atoms having 1, 2, or 3 non-hydrogen neighbors.

in a loop, selects a single SMILES entry, locks the row to prevent duplicate calculations, performs the force field optimization and DFT calculation, validate the resulting calculations, write results to the database, and repeat for a new molecule.

Data Records

The data set is provided in a chemical table file format, specifically an SDF molfile containing all optimized geometries with additional property fields including SMILES, Enthalpy, FreeEnergy, SCFenergy, AtomCharges, RotConstants, VibFreqs, and IRIntensity. All raw Gaussian M062X/def2TZVP logfiles for optimization and frequency calculations are also provided³⁴. Code to read the dataset and process the associated data in Python is provided in an associated github repository (<https://github.com/pstjohn/bde>). A description of the data fields in the SDF file are given in Table 1. In addition to the processed SDF file, raw Gaussian logfiles are provided in a separate zipped directory.

As molecules with more heavy atoms allow a greater number of possible arrangements, the database contains more examples of larger molecules than smaller molecules. A complete breakdown of the number of calculations in the database by number of heavy atoms is given in Table 2 and a breakdown of the formal radical center by element and degree is given in Table 3. Further characterization of the radical database to determine proximity of the radicals to stabilizing substituents. SMILES arbitrary target specification (SMARTS) patterns were used to determine whether each radical contains neighboring stabilizing features. Radicals are classified as allylic (adjacent to a C=C double bond), propargylic (adjacent to a C≡C triple bond), benzylic (adjacent to an aromatic carbon), adjacent to a π -acceptor group (an electron-withdrawing group, EWG), adjacent to a lone-pair (an electron-donating group, EDG), and captodative (alpha to both a π -acceptor and a lone-pair donor). Counts of radicals by neighboring substituents is given in Table 4.

As a set of consistent enthalpies between closed-shell molecules and radicals, this data has been used to calculate a large number of bond dissociation energies (BDEs)²⁸. With calculated bond strengths and 3D atomic structures of the parent molecules, we can examine bond strength vs. bond length curves for several common

Name	SMARTS	Count
Allylic	[#6;X3v3+0]-[#6]=[#6×3]	16,229
Propargylic	[#6;X3v3+0]-[#6]#[#6]	1,887
Benzylic	[#6;X3v3+0]-[c]	8,286
α -to π -acceptor	[#6;X3v3+0]-[C,N]=,[#N,O]	18,758
α -to lone-pair	[#6;X3v3+0]-[O,N]	55,136
Captodative	[#6;X3v3+0](-[O,N])-[C,N]=,[#N,O]	43,86

Table 4. Characterization of carbon-centered radicals by neighboring substituents.

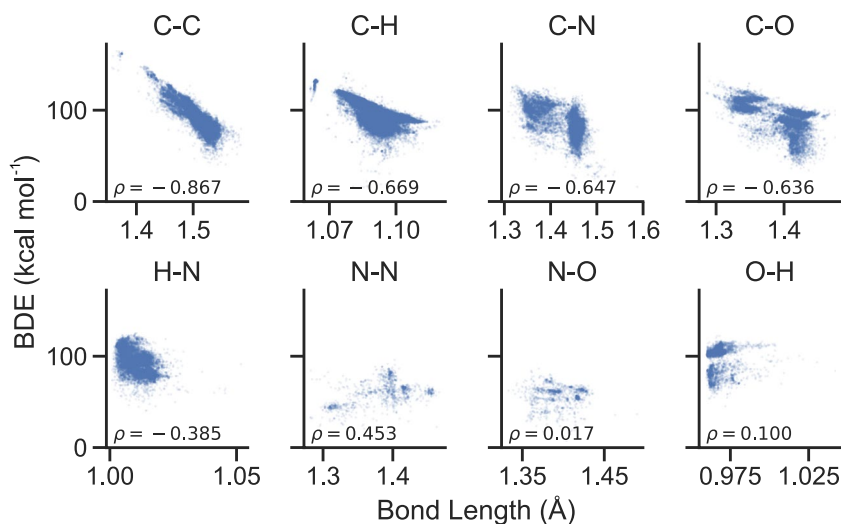


Fig. 2 Bond strength versus bond length for several common single bonds. Bond dissociation enthalpies are inversely correlated with bond lengths for carbon-containing bonds, but less so for other species.

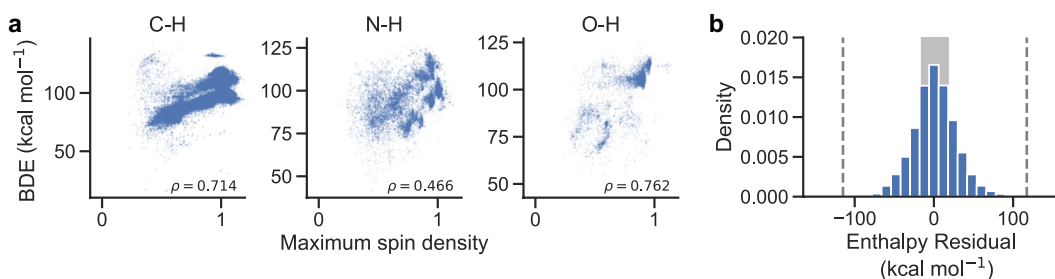


Fig. 3 Radical stabilization and enthalpy validation (a). BDE versus maximum atom spin density. Maximum spin density is calculated across all atoms in the resulting radical, with lower numbers indicating a more even distribution of electron spin across all atoms. (b) Distribution of calculated minus predicted enthalpies (in kcal mol⁻¹) following a linear model of atomic composition. The shaded grey region indicates the inner quartile range. Vertical grey dashed lines indicate the thresholds used for outlier detection, defined as ± 3 inner quartile ranges away from the first or third quartile.

single bonds. Figure 2 shows bond strengths versus bond lengths as calculated using this dataset. Correlation coefficients indicate that bond length vs. strength correlations are strongest for C–C single bonds, followed by similar, slightly weaker correlations for C–N, C–H, and C–O bonds. As expected, longer bond lengths are symptomatic of weaker dissociation enthalpies. In contrast, almost no correlation between bond length and strength exists for N–H, N–N, N–O or O–H bonds.

We also demonstrate how the dataset could also be used to investigate if radical stabilization (through delocalization of the resulting electron's spin density) affects bond strength. Figure 3a plots BDE versus the maximum spin density on any atom in the resulting radical for hydrogen atom abstraction reactions. For O–H and C–H bonds, there is a strong correlation ($\rho = 0.76$ and 0.71 , respectively) between maximum spin density and BDE, suggesting that radical delocalization plays an important role in determining bond enthalpies. However, for N–H bonds, correlations are much weaker.

Technical Validation

A series of convergence checks were performed to ensure the calculated enthalpies are as reliable as possible. Of the 322,871 total enthalpy calculations performed for this work, 30,327 (9.39%) were discarded due to various validation checks. Molecules with failures of any steps of the calculation pipeline, including the conformer embedding (5,079 molecules) and not reaching normal termination of the DFT calculations (2,213 molecules) were discarded. This was either due to a failure to converge the geometry optimization within the maximum number of steps of the Berny algorithm or due to a failure to converge the SCF procedure within the maximum number of cycles. Vibrational frequencies of the optimized molecules computed at the same level of theory as geometry optimization and were checked to ensure that the optimized stationary point was an energy minimum, with zero imaginary frequencies. If any frequencies were imaginary, the optimization was discarded (18,263 optimizations resulted in at least one imaginary frequency). The 3D structure of the resulting optimization was also inspected to ensure that the connectivity matched the Lewis structure of the input structure. The interatomic distances of formally bonded atom pairs were checked to ensure no bonds were greater than 0.4 Å plus the sum of the covalent radii of the two participating atoms (2,134 molecules failed the covalent radii check)³⁵. Finally, molecules were checked for an unreasonably high enthalpy per atom. A linear model was fit to each result's enthalpy, with the number of C, H, N, and O atoms as the independent variables. Residuals were close to normally distributed (Fig. 3b). Outliers were defined as those calculations that were more than 3 inner quartile ranges away from the first or third quartile. No molecules were outliers in the more stable direction, but 235 molecules had higher enthalpy residuals than the maximum cutoff, indicating they likely converged to highly unstable conformers and were removed.

Usage Notes

While the SDF file containing optimized geometry and extracted properties can be read with a number of different cheminformatic tools, we provide a simple example of processing the file with Python 3 and RDKit and using the data to calculate bond dissociation energies at <https://github.com/pstjohn/bde>.

Code availability

Code used to perform the high-throughput calculations are available at <https://github.com/pstjohn/bde>. The code relies on cclib and RDKit to process molecular information in Python, Gaussian to perform the DFT calculation, and pandas for data processing. Some of the code relating to the PostgreSQL database and NREL's HPC infrastructure is site-specific and will likely need to be altered to run these types of calculations on alternative HPC systems.

Received: 22 April 2020; Accepted: 30 June 2020;

Published online: 21 July 2020

References

- Cheng, G. J., Zhang, X., Chung, L. W., Xu, L. & Wu, Y. D. Computational organic chemistry: Bridging theory and experiment in establishing the mechanisms of chemical reactions. *J. Am. Chem. Soc.* **137**, 1706–1725 (2015).
- Messery, R. A. *et al.* Towards quantitative prediction of ignition-delay-time sensitivity on fuel-to-air equivalence ratio. *Combust. Flame* **214**, 103–115 (2020).
- Kim, S. *et al.* Experimental and theoretical insight into the soot tendencies of the methylcyclohexene isomers. *Proc. Combust. Inst.* **37**, 1083–1090 (2019).
- Atkinson, R. & Arey, J. Gas-phase tropospheric chemistry of biogenic volatile organic compounds: A review. *Atmos. Environ.* **37**, 197–219 (2003).
- Houmam, A. Electron transfer initiated reactions: Bond formation and bond dissociation. *Chem. Rev.* **108**, 2180–2237 (2008).
- Coote, M. L. In *Encyclopedia of Polymer Science and Technology* 3rd edn (ed. Kroschwitz, J. I.) *Computational Quantum Chemistry for Free-Radical Polymerization* (JohnWiley and Sons, 2004).
- Kim, S. *et al.* Computational Study of Bond Dissociation Enthalpies for a Large Range of Native and Modified Lignins. *J. Phys. Chem. Lett.* **2**, 2846–2852 (2011).
- Koniarczyk, J. L., Greenwood, J. W., Alegre-Requena, J. V., Paton, R. S. & McNally, A. A Pyridine–Pyridine Cross-Coupling Reaction via Dearomatized Radical Intermediates. *Angew. Chemie - Int. Ed.* **58**, 14882–14886 (2019).
- Gilmer, J., Schoenholz, S. S., Riley, P. F., Vinyals, O. & Dahl, G. E. Neural Message Passing for Quantum Chemistry. *arXiv:1704.01212* (2017).
- Faber, F. A. *et al.* Prediction Errors of Molecular Machine Learning Models Lower than Hybrid DFT Error. *J. Chem. Theory Comput.* **13**, 5255–5264 (2017).
- Schütt, K. T., Arbabzadah, F., Chmiela, S., Müller, K. R. & Tkatchenko, A. Quantum-chemical insights from deep tensor neural networks. *Nat. Commun.* **8**, 13890–13898 (2017).
- Battaglia, P. W. *et al.* Relational inductive biases, deep learning, and graph networks. *arXiv:1806.01261 cs.LG* (2018).
- Kearnes, S., McCloskey, K., Berndl, M., Pande, V. & Riley, P. Molecular graph convolutions: moving beyond fingerprints. *J. Comput. Aided. Mol. Des.* **30**, 595–608 (2016).
- Smith, J. S., Isayev, O. & Roitberg, A. E. ANI-1: an extensible neural network potential with DFT accuracy at force field computational cost. *Chem. Sci.* **8**, 3192–3203 (2017).
- Sinititskiy, A. V. & Pande, V. S. Deep Neural Network Computes Electron Densities and Energies of a Large Set of Organic Molecules Faster than Density Functional Theory (DFT). *arXiv:1809.02723* (2018).
- St. John, P. C., Guan, Y., Kim, Y., Kim, S. & Paton, R. S. Prediction of organic homolytic bond dissociation enthalpies at near chemical accuracy with sub-second computational cost. *Nat. Commun.* **11**, 1–12 (2020).
- Grambow, C. A., Li, Y.-P. & Green, W. H. Accurate Thermochemistry with Small Data Sets: A Bond Additivity Correction and Transfer Learning Approach. *J. Phys. Chem. A* **123**, 5826–5835 (2019).
- Álvarez-Moreno, M. *et al.* Managing the computational chemistry big data problem: The ioChem-BD platform. *J. Chem. Inf. Model.* **55**, 95–103 (2015).
- Ramakrishnan, R., Dral, P. O., Rupp, M. & von Lilienfeld, O. A. Quantum chemistry structures and properties of 134 kilo molecules. *Sci. Data* **1**, 191–197 (2014).
- Smith, J. S., Isayev, O. & Roitberg, A. E. Data Descriptor: ANI-1, A data set of 20 million calculated off-equilibrium conformations for organic molecules. *Sci. Data* **4**, 1–8 (2017).

21. Grambow, C., Pattanaik, L. & Green, W. H. Reactants, Products, and Transition States of Elementary Chemical Reactions Based on Quantum Chemistry. *ChemRxiv. Preprint*, <https://doi.org/10.26434/chemrxiv.11400240.v2> (2019)
22. Rupp, M., Tkatchenko, A., Müller, K.-R. & von Lilienfeld, O. A. Fast and Accurate Modeling of Molecular Atomization Energies with Machine Learning. *Phys. Rev. Lett.* **108**, 058301 (2012).
23. Smith, J. S., Nebgen, B., Lubbers, N., Isayev, O. & Roitberg, A. E. Less is more: Sampling chemical space with active learning. *J. Chem. Phys.* **148** (2018).
24. Smith, J. S. *et al.* Approaching coupled cluster accuracy with a general-purpose neural network potential through transfer learning. *Nat. Commun.* **10**, 2903 (2019).
25. Kim, S. *et al.* PubChem 2019 update: improved access to chemical data. *Nucleic Acids Res.* **47**, D1102–D1109 (2018).
26. Zhao, Y. & Truhlar, D. G. The M06 suite of density functionals for main group thermochemistry, thermochemical kinetics, noncovalent interactions, excited states, and transition elements: two new functionals and systematic testing of four M06-class functionals and 12 other function. *Theor. Chem. Acc.* **120**, 215–241 (2007).
27. Frisch, M. J. *et al.* Gaussian 16 Rev. C.01. *Gaussian 16* (2016).
28. John, P. S. *et al.* BDE-db: A collection of 290,664 Homolytic Bond Dissociation Enthalpies for Small Organic Molecules. *figshare* <https://doi.org/10.6084/m9.figshare.10248932.v1> (2019).
29. Landrum, G. A. RDKit: Open-source cheminformatics, <http://www.rdkit.org> (2020).
30. Halgren, T. A. Merck molecular force field. I. Basis, form, scope, parameterization, and performance of MMFF94. *J. Comput. Chem.* **17**, 490–519 (1996).
31. Riniker, S. & Landrum, G. A. Better Informed Distance Geometry: Using What We Know To Improve Conformation Generation. *J. Chem. Inf. Model.* **55**, 2562–2574 (2015).
32. O'Boyle, N. M. *et al.* Open Babel: An open chemical toolbox. *J. Cheminform.* **3**, 33 (2011).
33. O'Boyle, N. M., Tenderholt, A. L. & Langner, K. M. cclib: A library for package-independent computational chemistry algorithms. *J. Comput. Chem.* **29**, 839–845 (2008).
34. St John, P. C. *et al.* Quantum chemical calculations for over 200,000 organic radical species and 40,000 associated closed-shell molecules. *figshare* <https://doi.org/10.6084/m9.figshare.c.4944855> (2020).
35. Cordero, B. *et al.* Covalent radii revisited. *Dalt. Trans.* 2832–2838 (2008).

Acknowledgements

We thank Kristin Munch for helpful conversations and assistance setting up the PostgreSQL database. Computational resources for P. C. St. John, Y. Kim, and S. Kim were provided by the Computational Sciences Center at National Renewable Energy Laboratory. R.S.P. gratefully acknowledges the RMACC Summit supercomputer supported by the National Science Foundation (ACI-1532235 and ACI-1532236), the University of Colorado Boulder and Colorado State University; the Extreme Science and Engineering Discovery Environment (XSEDE) through allocation TG-CHE180056. This work was authored in part by the National Renewable Energy Laboratory, operated by Alliance for Sustainable Energy, LLC, for the U.S. Department of Energy (DOE) under Contract No. DE-AC36-08GO28308. Funding provided by U.S. Department of Energy Office of Energy Efficiency and Renewable Energy under the Co-Optima initiative. The views expressed in the article do not necessarily represent the views of the DOE or the U.S. Government. The U.S. Government retains and the publisher, by accepting the article for publication, acknowledges that the U.S. Government retains a nonexclusive, paid-up, irrevocable, worldwide license to publish or reproduce the published form of this work, or allow others to do so, for U.S. Government purposes.

Author contributions

P.C.S. implemented the high-throughput calculation pipeline, collected the results, and wrote the initial manuscript draft. Y.K. designed the calculation pipeline and calculated proof-of-concept results. All authors designed parts of the validation workflow. All authors participated in planning the study and editing the final manuscript.

Competing interests

The authors declare no competing interests.

Additional information

Correspondence and requests for materials should be addressed to P.C.S., S.K. or R.S.P.

Reprints and permissions information is available at www.nature.com/reprints.

Publisher's note Springer Nature remains neutral with regard to jurisdictional claims in published maps and institutional affiliations.



Open Access This article is licensed under a Creative Commons Attribution 4.0 International License, which permits use, sharing, adaptation, distribution and reproduction in any medium or format, as long as you give appropriate credit to the original author(s) and the source, provide a link to the Creative Commons license, and indicate if changes were made. The images or other third party material in this article are included in the article's Creative Commons license, unless indicated otherwise in a credit line to the material. If material is not included in the article's Creative Commons license and your intended use is not permitted by statutory regulation or exceeds the permitted use, you will need to obtain permission directly from the copyright holder. To view a copy of this license, visit <http://creativecommons.org/licenses/by/4.0/>.

The Creative Commons Public Domain Dedication waiver <http://creativecommons.org/publicdomain/zero/1.0/> applies to the metadata files associated with this article.

© The Author(s) 2020